EL-FERMAOUI, A.
Pincock, Allen & Holt, Tucson, Arizona, U.S.A.
NOWATZKI, E.
University of Arizona, Tucson, Arizona, U.S.A.

Effect of Confining Pressure on Performance of Geotextiles in Soils

L'effet de la pression de confinement sur la performance de géotextiles enterrés

The purpose of this research was to study the effect of confining stress and soil support and cover materials on tensile strength characteristics of geotextiles. This has direct application to the equivalent tensile stress and type of failure of the geotextiles when embedded in the ground.

The effect of varying the type of support and cover materials on the stress-strain relationships of two different geotextiles, Polyfilter X (woven) and Mirafi 140S (nonwoven), were investigated for normal stresses of 47.9 kPa (0.5 tsf), 95.8 kPa (1 tsf), 191.6 kPa (2 tsf) and 383.2 kPa (4 tsf). It was found that, in general, the "equivalent tensile stress" at failure increased with increasing confining stress.

Equations for the stress-strain curves and for the tangent moduli as a function of normal stress were derived for Polyfilter X and a dry sand/sand support/cover combination. The expressions developed may be used directly in finite element models of soil-fabric structure interactions. The procedure described may be used for other combinations of geotextile and support/cover materials to develop similar relationships.

Le but de cette recherche était d'étudier l'effet de la pression de confinement du support des sols et des matériaux de couverture sur les caractéristiques de tension de géotextiles. Une application directe de cette étude est la définition de la tension équivalente et du type de rupture des géotextiles enterrés.

L'effet de la variation du type de support et matériau de couverture sur la relation force-tension de deux géotextiles différents, Polyfilter X (tissé) et Mirafi 140S (non tissé) a été observé pour des tensions normales de 47.9 kPa (0.5 tsf), 95.8 kPa (1 tsf), 191.6 kPa (2 tsf), et 383.2 kPa (4 tsf). Un résultat général est que la "tension équivalente" de rupture s'accroit avec la tension de confinement.

Les équations donnant les courbes force-tension et les modules de tangente en fonction de la tension normale ont été etablies pour le cas de Polyfilter X couvert et supporté par un mélange de sable sec et sable ordinaire. Les formules ainsi trouvées, pouvant s'employer directement dans un modèle à éléments finis de l'interaction sol-structure en géotextile. L'approche peut s'employer à l'étude d'autres combinaisons de géotextiles et matériau de support/couverture, conduisant à des formules semblables.

INTRODUCTION

Currently, geotextiles are mostly used as a reinforcement material to improve a weak soil's load-bearing capacity. The mechanism developed by the use of the geotextiles as a reinforcement material is a function of the stress distribution due to the interface friction between the geotextile and the soil. Theoretically, the geotextile, when embedded in soil, is considered to be a pinned beam so that horizontal and vertical movements at the extremities are prevented. Rotation is allowed so that tension in the geotextile is developed as loads are applied. Practically, in order to design geotextile-reinforced systems, the effect of soil confinement and other placement factors on the performance of the geotextile must be evaluated. This research provides an insight into the effect of soil confinement, cover and support materials and soil moisture content, on the tensile strength parameters of selected geotextiles.

TESTING EQUIPMENT, MATERIALS AND TESTING PROCEDURES

Testing Equipment and Materials

Sample Box

A specially designed sample box was used in conjunction with a direct shear device to perform geotextile tensile tests. The box was made up of two sections which can be connected together with screws similar to a conventional direct shear device shear box. (Fig. 1). The spacing between the two sections of the box can be adjusted to allow the placement of a geotextile specimen in the horizontal plane between the support material (at the bottom) and the cover material (at the top). When assembled, the box was a square with interior side dimensions of 6.35 cm (2.5 in.) and a height of 3.81 cm (1.5 in.). A square cover plate slightly less than 6.35 cm on a side, was

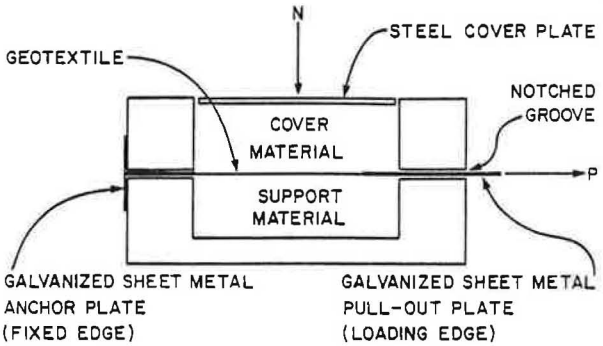

Fig. 1 Sample box for tensile tests.

placed on the top surface of the cover material. This cover plate distributed the normal load (N) from the test device uniformly over the soil material contained in the box.

Geotextile Specimen

To make sure the geotextile specimen received a uniformly distributed normal pressure from the vertical load head, it was cut in a 5.08 cm (2 in.) square. Thus the geotextile specimen could be placed in the box in such a way that it would be confined under the normal stress during the entire loading sequence up to 25% strain or until failure. The loading side of the specimen and its opposite extremity were glued and rivetted between two thin pieces of sheet metal that formed a type of clip (Fig. 1). The pull-out plate on the loading edge was connected to the horizontal loading arm of the direct shear device through which the tensile load (P) was applied. The opposite extremity was fixed to the far side of the box.

Materials Used

Two types of geotextiles were studied: woven and nonwoven. Three kinds of woven geotextile were tested: Polyfilter X, Mirafi 100X and Mirafi 500X. The nonwoven geotextiles tested were Mirafi 140S, Typar 3601, and Bidim C-34. Tests were performed with confinement oriented along grain and across the grain for each of the fabrics.

Sand and gravel were used as the confinement materials. The sand was #30 Ottawa sand having an approximate dry density, γ_d, of 14.13 kN/m^3 (90 pcf). The gravel was a fine river run gravel having uniform gradation and an approximate dry density, γ_d, of 16.96 kN/m^3 (108 pcf).

Testing Procedures

For "dry tests", the geotextile specimens were placed on top of the air dried support material which was placed into the bottom half of the sample box at a predetermined dry density (γ_d = 14.13 kN/m^3 for #30 Ottawa sand; γ_d = 16.96 kN/m^3 for fine gravel). The top half of the sample box was then positioned over the bottom half and fastened by hand-tightening the connecting screws. Care was exercised in placing the geotextile specimen so that the sheet metal pull-out plate and anchor plate fit in the grooves notched into the upper and lower portions of the box. The air dried cover material was then introduced into the top half of the sample box. If the support and cover materials were the same, the materials were placed at the same dry density. After the metal cover plate was placed on the top of the cover material, the loading head of the test device was lowered to make contact with it. Following application of the normal load, the sheet metal connector was attached to the horizontal loading arm of the direct shear device and the test begun.

For "wet tests", the soil and geotextile test specimens were prepared in the same way as for the "dry tests", except that after attachment of the pull-out plate to the direct shear device loading arm, the samples were soaked in water for 24 hours before testing.

All pull-out tests were performed at a horizontal displacement rate of 1.27 mm/min. (0.05 in./min.). The first reading of pull-out load was recorded for a horizontal displacement of 0.254 mm (0.01 in.). Thereafter, readings of pull-out load were recorded for 0.508 mm (0.02 in.) increments until 5.08 mm (0.2 in.) of deformation occurred; then readings were taken at 1.27 mm (0.05 in.) increments until 12.70 mm (0.5 in.) of total horizontal deformation occurred. By using this procedure, the low stress range of the stress-strain (load-deformation) curve was well defined. All specimen-soil combinations shown in Table 1, were tested at normal stresses of 47.9 kPa (0.5 tsf), 95.8 kPa (1 tsf), 191.6 kPa (2 tsf), and 383.2 kPa (4 tsf).

In this study, field conditions were simulated in the laboratory by keeping the entire geotextile confined under the normal pressure during horizontal loading until failure of the geotextile or 25% strain occurred. Also, the geotextile sample was free to deform transversely so that necking could occur in the portion of the sample that was under normal stress just as it could occur in the field.

Table 1: Summary of Testing Program

Each series included tests at normal stresses of 0 kPa, 47.9 kPa (0.5 tsf), 95.8 kPa (1 tsf), 191.6 kPa (2 tsf) and 383.2 kPa (4 tsf). All soils were air dry except where noted.

Geotextile Type	Sand-Sand Interface	Gravel-Sand Interface	Gravel-Gravel Interface
Woven			
Polyfilter X	X[a]	X	X
Mirafi 100X	X	-	-
Mirafi 500X	X	-	-
Nonwoven			
Mirafi 140S	X[a]	X	X
Typar 3601	X	-	-
Bidim C-34	X	-	-

[a] Tests were also performed for wet interfaces.

PRESENTATION AND DISCUSSION OF TEST RESULTS

Stress-strain curves were used to evaluate the tensile strength characteristics of the geotextiles tested. To develop such curves, plots of the variation of sample width versus loading deformation for each of the geotextiles were obtained under conditions of zero confining stress (Fig. 2). It was assumed that the thickness of the specimen did not change during loading, even in the reduced section. It was also assumed that the amount of necking of the confined geotextile at a given horizontal deformation was the same as that of the unconfined geotextile at the same horizontal deformation.

Under normal stress, σ_n, when the fabric was pulled out, shear stresses were mobilized along the surface area of the geotextile sample. The magnitude of the interface shear stress, τ, is equal to $c + \sigma_n \tan \phi$; where c and ϕ are the interface adhesion and the friction angle, respectively, between the

confining material and the geotextile. However, because the displacements are variable along the length of the fabric, the shear stresses are not uniformly distributed.

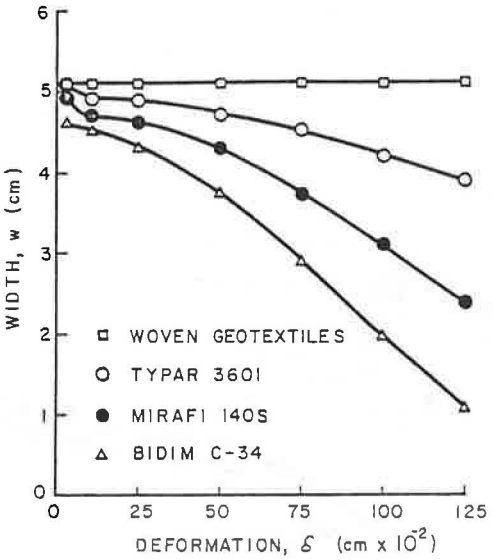

Fig. 2 Geotextile specimen widths versus horizontal deformation (unconfined loading).

Figure 3 shows a schematic of the way in which interface shear stresses acting on the geotextile specimen were assumed to develop. Immediately after application of the horizontal force P by the direct shear device, shear stresses began to be mobilized on the geotextile-soil interfaces. These shear stresses (τ_{st} on the top and τ_{sb} on the bottom) are due to the applied normal stress. The equilibrium length, L_e, is that portion of the geotextile where shear stresses become mobilized under a certain normal stress for a given horizontal load of magnitude P. Initially, there will be no movement and no tensile stress in the geotextile in length L which is beyond L_e (Fig. 3). The distribution of τ_{st} and τ_{sb} is not uniform even within L_e. Summation of the horizontal forces shown in Figure 3a yields $(\tau_{st} + \tau_{sb})A_{fe} = P$; where $A_{fe} = L_e$ times the average lateral width of the fabric (W_{avg}). If a cross-section A-A is cut at a length L_c less than L_e, the force equilibrium expression from Figure 3b is $(\tau_{st} + \tau_{sb})A_{fc} + T_G = P$: where $A_{fc} = L_c \times W_{avg}$, and T_G = geotextile tensile force. When the applied horizontal load P reaches its ultimate value, full interface shearing resistance becomes mobilized along the total surface area of the geotextile, and the geotextile sample moves as a whole. At this point it is reasonable to assume a uniform shear stress distribution along the interface due to the reorientation of the soil particles. If the support and cover materials are the same, then $\tau_{st} = \tau_{sb}$. The galvanized sheet metal surfaces were very smooth, and the shear stresses developed along them due to the normal stresses were assumed to be very small compared to the shear stresses developed on the geotextile-soil interface. Therefore, the mobilized shear stresses along the sheet metal-soil interface were neglected.

Equivalent tensile stresses (σ_T) under various normal stresses (σ_n) were obtained by dividing the geotextile stretch-out load (P) by the cross-sectional area of the geotextile. Equivalent tensile stresses are plotted in Figures 4 through 7 at 5% strain increments for the sake of clarity; but the stress-strain curves themselves were drawn using intermediate points as well.

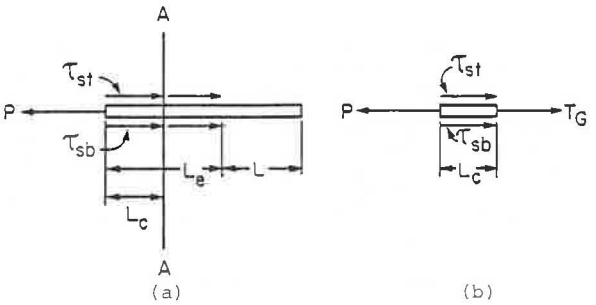

Fig. 3 Horizontal forces and interface shear stresses acting on geotextile specimen.
(a) Mobilization of the shear stresses
(b) Cross-section A-A

EQUIVALENT TENSILE STRESS OF GEOTEXTILES

The width of all woven geotextiles remained virtually constant during tensile testing without soil in the sample box (Fig. 2). Therefore, stress-strain curves were determined for constant cross-section at all stress levels. The width of all nonwoven geotextiles, however, diminished during tensile testing and subsequently failed by necking (Fig. 2). Therefore, stress-strain curves were determined for reduced cross sections depending upon the amount of displacement (strain) attained during the test. The equivalent tensile stress (σ_T) was obtained by dividing the geotextile stretch-out load by the cross sectional area of geotextile.

RESULTS SHOWING EFFECT OF COVER AND SUPPORT MATERIALS ON EQUIVALENT TENSILE STRESS

When both cover and support materials were dry #30 Ottawa sand, high shear stresses were mobilized along the geotextile-soil interface due to the application of normal stress. For the case of the geotextile confinement under dry #30 Ottawa sand as cover material and dry fine gravel as support material, there was less surface contact on the geotextile-gravel interface than on the geotextile-sand interface. Thus, there was less shear stress mobilization along the geotextile-gravel interface than along the geotextile-sand interface. The net result was a reduction in the equivalent tensile stresses as shown in Figures 4 and 5 for one type of woven fabric and one type of nonwoven fabric, respectively, under 383.2 kPa (4 tsf) normal stress. Also,

it is noticed from these two figures that the geotextile gravel-gravel interface exhibited the lowest equivalent tensile stresses as compared to the other geotextile-material combinations due to the lowest surface contact at the interface and thus less mobilization of shear stress.

RESULTS SHOWING EFFECT OF MOISTURE CONTENT

The fibers used to make fabrics are generally hydrophobic. Therefore, they are relatively insensitive to moisture regain. The tensile strength for the woven and nonwoven geotextiles tested with wet #30 Ottawa sand as cover and support materials was the same as for the dry case under zero normal stress. However, when woven geotextiles were tested with normal stresses applied to wet cover and support materials, it appeared that some water was retained on the geotextile-soil interface during testing, probably due to the rough surface of the woven fabric. This wet geotextile-soil interface caused the geotextile to slip slightly. Thus shear stresses mobilized on the geotextile interface decreased with a corresponding reduction in the equivalent tensile stresses (Fig. 4). The equivalent tensile stress reduction, at 25% ε, was approximately 30%.

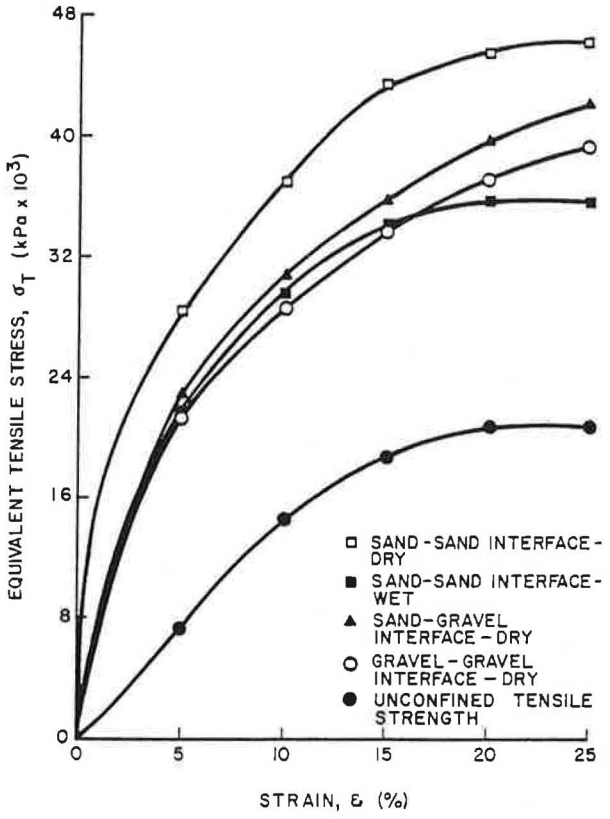

Fig. 4 Stress-strain curves for Polyfilter X (woven fabric) under 383.2 kPa (4 tsf) normal stress for various combinations of cover and support materials.

Additionally, nonwoven geotextiles tested under wet conditions sometimes displayed slightly higher equivalent tensile stresses under increased normal stresses than when they were tested under dry conditions (Fig. 5). This may be due to the "wick" action of the geotextile in draining moisture from the soil near the interface. The resulting increase in effective stresses in the soil could cause the cover and support materials to densify in the area of the geotextile and lead to the observed almost 5% increase in the equivalent tensile stress.

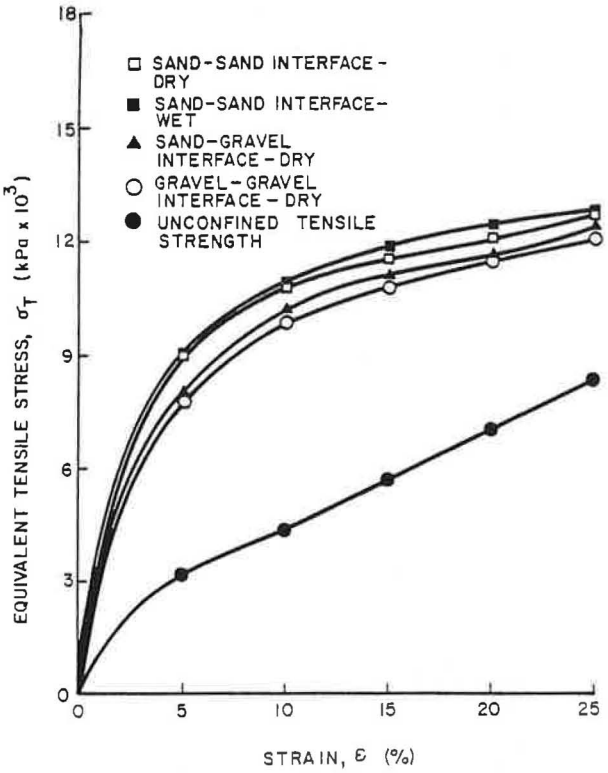

Fig. 5 Stress-strain curves for Mirafi 140S (nonwoven fabric) under 383.2 kPa (4 tsf) normal stress for various combinations of cover and support materials.

RESULTS SHOWING EFFECT OF NORMAL STRESS ON EQUIVALENT TENSILE STRESS

Stress-strain curves for Polyfilter X woven fabric and Mirafi 140S nonwoven fabric (support and cover material = dry #30 Ottawa sand) are shown in Figures 6 and 7 respectively, for various normal stresses. High shear stresses were mobilized along the geotextile-soil interface due to the application of normal stresses. This is clearly noticed in the two stress-strain figures especially in Figure 6 where a significant increase in the equivalent tensile stress can be noted for even a relatively small normal stress of 47.9 kPa (0.5 tsf) as compared to the unconfined specimen. The higher the normal stress, the

higher the equivalent tensile stress at the same strain level. The results for all the other geotextile-sand combinations followed the same pattern.

Almost all the stress-strain curves of the geotextiles exhibited an initial linear portion until approximately 0.5% strain level. In addition, all curves have identical tangent moduli after about 20% strain regardless of the type of geotextile or the magnitude of normal stresses. As indicated previously, it is felt that this is due to the full and even mobilization of all the shearing stresses on the geotextile-soil interfaces.

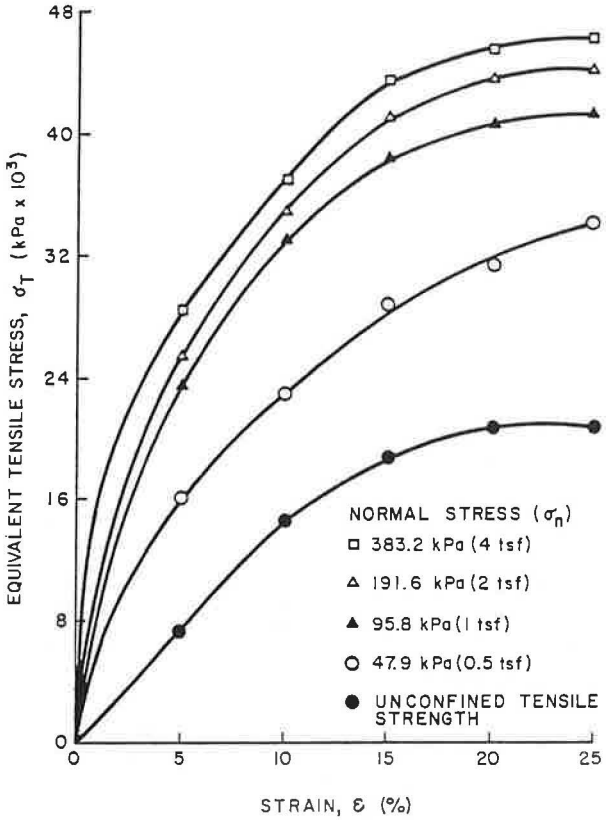

Fig. 6 Stress-strain curves for Polyfilter X (woven fabric); support and cover material = dry #30 Ottawa sand.

RELATIONSHIP BETWEEN TANGENT MODULUS (E_t) AND NORMAL STRESS (σ_n)

Because problems involving geotextile-soil interactions are often modelled and solved by the finite element method (FEM), an equation was developed for the stress-strain curves and for the tangent modulus (E_t) as a function of the normal stress (σ_n), following a procedure from Duncan and Chang (1). The initial tangent moduli (E_i), of the stress-strain curves under the various normal stresses, were computed and plotted versus their corresponding normal stresses (σ_n), as shown in Figure 8 for

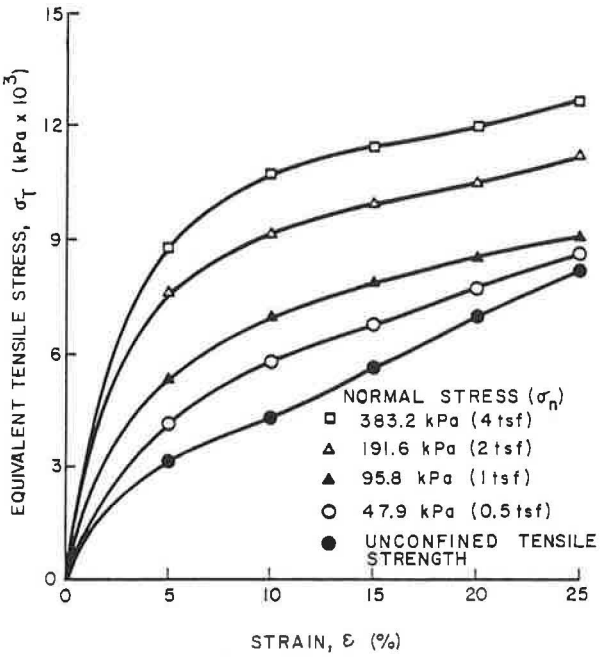

Fig. 7 Stress-strain curves for Mirafi 140S (nonwoven fabric); support and cover material = dry #30 Ottawa sand.

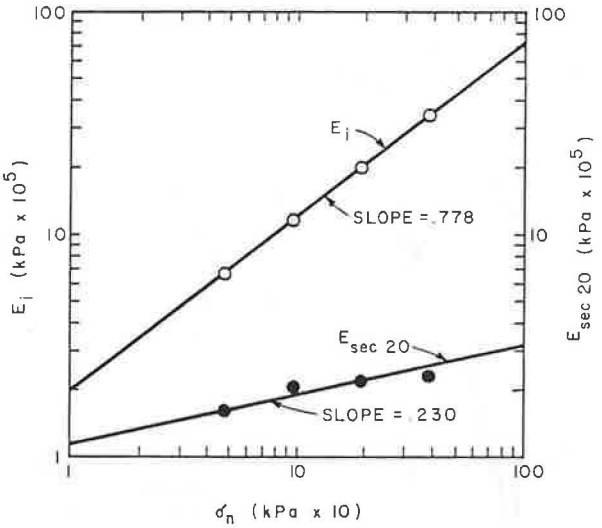

Fig. 8 Log E_i and log E_{sec20} versus log σ_n for Polyfilter X (woven fabric); cover and support material = dry #30 Ottawa sand.

Polyfilter X fabric. In addition, the secant moduli (E_{sec}), of the stress-strain curves at 20% strain were computed and plotted versus their corresponding normal stresses. Two straight lines were obtained: one for E_i, and one for E_{sec20}. These straight lines indicate that E_i and E_{sec20} increase linearly on log-log paper with increasing normal stresses. If the

slope of the E_i line and its y-intercept are called q and k, respectively, the following equation can be written:

$$\text{Log } E_i = q \log \sigma_n + \log k \qquad (1)$$

This equation is solved for initial tangent modulus to yield:

$$E_i = k(\sigma_n)^q \qquad (2)$$

To obtain a better definition of E_i, ε/σ_T was plotted versus ε as shown in Fig. 9 for Polyfilter X and for σ_n = 47.9 kPa (0.5 tsf) and σ_n = 383.2 kPa (4 tsf). The inverse of ε/σ_T at the intercept gives the initial tangent modulus for its corresponding normal stress. For normal stresses between 47.9 kPa and 383.2 kPa, linear interpolation between the straight lines shown in Fig. 9 is valid to find the E_i value. A break in the straight line curve exists at small strain levels for both normal stresses. Therefore, each curve is

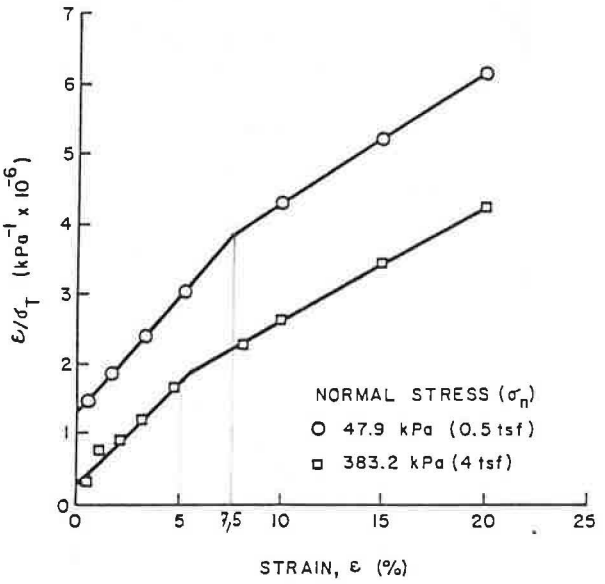

Fig. 9 ε/σ_T versus ε for Polyfilter X (woven fabric); support and cover material = dry #30 Ottawa sand.

approximated by two straight line segments with different slopes and y-intercepts. The slopes and y-intercepts of the straight lines are represented in Table 2 for Polyfilter X. Values

Table 2

Slope (m) and y-intercept (b) values for the straight lines of Figure 9.

σ_n(kPa)	ε	m (kPa^{-1})	b (kPa^{-1})
47.9	$0 < \varepsilon < .075$	31.90×10^{-6}	1.31×10^{-6}
	$.075 < \varepsilon < .20$	18.13×10^{-6}	2.32×10^{-6}
383.2	$0 < \varepsilon < .05$	29.01×10^{-6}	$.29 \times 10^{-6}$
	$.05 < \varepsilon < .20$	15.95×10^{-6}	1.02×10^{-6}

for these parameters could be obtained for any combination of geotextile and cover/support materials by using the same procedure as outlined above. The general equation of any straight line on the axes shown in Fig. 9 is:

$$\frac{\varepsilon}{\sigma_T} = m\varepsilon + b \qquad (3)$$

where m and b are the slope and y-intercept, respectively.

Solving Equation 3 for σ_T, gives:

$$\sigma_T = \frac{\varepsilon}{m\varepsilon + b} \qquad (4)$$

which is the general equation for the stress-strain curves of Fig. 6. Since the tangent modulus (E_t) is the derivative of σ_T with respect to ε, Equation 4 may be expressed as follows:

$$E_t = \frac{d\sigma_T}{d\varepsilon} = \frac{m\varepsilon + b - m\varepsilon}{(m\varepsilon + b)^2} = \frac{b}{(m\varepsilon + b)^2} \qquad (5)$$

But at $\varepsilon = 0$, $E_t = E_i = \frac{1}{b}$

and from Equation 2: $E_i = k(\sigma_n)^q$

$$\text{Therefore } b = \frac{1}{E_i} = \frac{1}{k(\sigma_n)^q} = \frac{1}{k}(\sigma_n)^{-q} \qquad (6)$$

This expression for b, when substituted into Equation 5, yields the following general expression for E_t as a function of applied normal stress and strain level:

$$E_t = \frac{\frac{1}{k}(\sigma_n)^{-q}}{(\frac{1}{k}(\sigma_n)^{-q} + m\varepsilon)^2} \qquad (7)$$

Equation 7 relates the mechanical properties of the geotextile with the normal stress under which the geotextile is embedded; therefore, it is useful for design analysis in the soil-geotextile reinforcement systems in which the geotextile becomes an interactive stress-carrying component of the system. Simple laboratory tests such as those described previously can be used to determine the constants K and q for various combinations of cover and support soils-geotextile type and moisture conditions.

ACKNOWLEDGMENTS

The authors wish to thank Mr. Lutz Kunze and his staff at Pincock, Allen & Holt, Inc., Tucson, Arizona for help in reviewing the manuscript and providing support in the form of word processing and drafting services.

REFERENCES

(1) DUNCAN, J.M. and C.Y. CHANG, "Nonlinear Analysis of Stress and Strain in Soils", Journal of the Soil Mechanics and Foundations Division, ASCE, Vol. 96, No. SM9, Proceedings Paper 7513, September 1970, pp. 1635-1653.